Phys. Status Solidi A **210,** No. 5, 1006–1012 (2013) / **DOI** 10.1002/pssa.201200781

Part of Special Section on
Engineering of Functional Interfaces

physica status solidi a
www.pss-a.com
applications and materials science

Vapour phase co-deposition of Al–Cu thin film alloys

Martina Hafner, Andrei Ionut Mardare, and Achim Walter Hassel*

Institute for Chemical Technology of Inorganic Materials, Johannes Kepler University Linz, Altenberger Str. 69, 4040 Linz, Austria

Received 30 September 2012, revised 20 December 2012, accepted 23 March 2013
Published online 6 May 2013

Keywords Al–Cu, microstructure, thermal evaporation, thin film

* Corresponding author: e-mail achimwalter.hassel@jku.at, Phone: +43 732 2468 8700, Fax: +43 732 2468 8905

The fabrication and characterisation of Al–Cu thin film alloys obtained using co-deposition geometry from individual Al and Cu sources were addressed. A compositional gradient ranging from 36 to 93 at.% Cu was obtained. The surface microstructure evolved with a strong influence on the Cu content. This was connected to the presence of the Cu(111) in the alloys. The electrical resistivity showed a decrease by almost one order of magnitude in the Cu rich region of the Al–Cu combinatorial library. Al–Cu thin films evaporated from a single source produced a surface compositional gradient of 7 at.%. X-ray photoelectron spectroscopy (XPS) depth profiling revealed an in-depth compositional gradient as well. This behaviour was attributed to the gas phase dynamics of Al and Cu during the thin film formation.

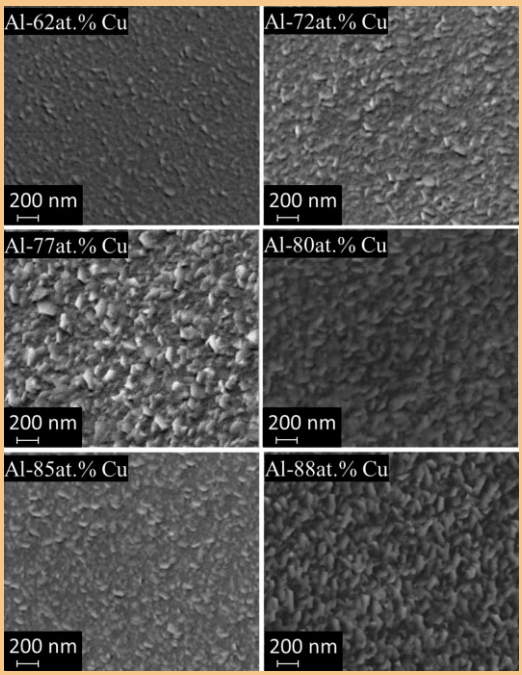

1 Introduction In modern thin film technology Al plays an important role in various applications. One of the major applications is found in the micro-electronic industry due to the low cost of Al thin film fabrication and its straight forward film formation mechanism. Thermal evaporation using either Joule heating or electron beam processing produces high quality films with a good control of the evaporation rate which allows a proper control of the adhesion to the substrate [1, 2]. One major problem was identified in the hillock formation which appears at very low deposition rates [3]. The hillock formation was also identified during deposition of Al–Cu thin film alloys with strong temperature dependence [4, 5]. Alloying with Cu decreased the electromigration effects when used as interconnects or conductive lines in micro-electronics [6] as compared to the case of using pure Al or pure Cu thin films [7]. A lot of effort is presently made for further improving the performance of the Al–Cu thin film interconnects (e.g. by

optimising the substrate surface) while decreasing their thickness to become compatible with the sub-0.13 μm technology [8, 9].

Al–Cu alloys are a technically important material class in which the Cu compound is used to harden the light and soft aluminium. The formation of secondary phase particles is not only responsible for this hardening but also leads to filiform corrosion e.g. in alloys such as AA2024 [10]. A systematic electrochemical study has been performed on a composition spread Al–Cu material library showing that a certain threshold of Cu content is necessary to make oxygen evolution on this passive material possible [11].

The needs for modern flexible electronics attracted interest in using Al and Al–Cu thin films directly on plastic substrates [12]. Combined with local electrochemical oxidation, these films have shown great potential for applications in flexible thin film capacitors and transistors [13, 14]. Very good mechanical properties have been identified during tensile testing of Al–Cu thin films on plastic substrates, the strength being improved by one order of magnitude as compared to the equivalent bulk material due to the decreased grain size [15].

Al–Cu thin film formation depends on the deposition method used. Multilayer formation followed by thermal annealing has shown the presence of internal friction during the interdiffusion process, always forming the Al_2Cu phase on the surface of the film structure [16]. Nevertheless, the thermal diffusion technique has proven to be an effective process for obtaining Al–Cu thin film alloys [17]. Reactive phase formation of Al–Cu thin film alloys has shown formation of intermetallics at temperatures above 50 °C as a function of composition [18]. Co-evaporation from separate elementary sources was successfully applied for the deposition of Al-based alloys [19]. In this work, single source alloy and co-deposition from individual sources are investigated and compared for a better understanding of the Al–Cu thin film formation process.

2 Experimental details In order to investigate the properties of Al–Cu thin film alloys, two different approaches were used. The properties of films obtained from vapour phase deposition using a single Al–Cu source were compared with the ones obtained by co-deposition from individual Al and Cu sources. The raw materials used for the individual sources during the Al–Cu co-deposition were high purity Al and Cu pellets (>99.95%). For the single source Al–Cu depositions, self-cast bulk Al–Cu alloys were used. The fabrication of the bulk alloys was done using a pivotable induction furnace (Linn – High Therm) with a maximum power of 10 kW. High purity (>99.95%) Al and Cu pellets in the correct proportions were mixed for obtaining a final alloy composition of Al-72.4 at.% Cu. Before melting, the furnace chamber was evacuated down to 1.0 Pa for removing the oxygen. Varigon® H6 gas (Linde) was used several times to flush the chamber before the heating process started in order to avoid oxide formation during the melting process. Heating up to 1200 °C ensured a complete melting and mixing of both Al and Cu in the liquidus phase. As soon as both materials were molten, the furnace chamber was manually brought to a vertical position using its pivotal function in order to cast the material into a stainless steel mould. In this way, homogeneous Al–Cu ingots ($20 \times 20 \times 200\,mm^3$) were produced. At a later stage, small pellets (approximately $10\,mm^3$) were mechanically machined from the ingot for serving as sources for thin film depositions.

The Al–Cu thin films were deposited on a set of 16 borosilicate microscope slide substrates ($15 \times 15\,mm^2$) covering the equivalent area of a 10 cm diameter Si wafer using a self constructed multiple sources thermal evaporator. The system consisted of a steel vacuum chamber with a base pressure of 10^{-4} Pa and a pneumatically detachable bottom flange containing high current feedthroughs made from pure Cu. Independent DC power sources (2 kW each) are used for providing the electrical energy necessary for the Joule heating in each of the evaporation sources. High resolution crystal quartz balances (with a noise level below $0.003\,nm\,s^{-1}$) placed directly above each thermal source were used for *in situ* monitoring of the evaporation process. An in-house developed LabView software with an integrated PID controller was employed for controlling the power sources using the feedback input from the thickness monitors. In this way, the evaporation rate of each material could be directly and independently controlled through the corresponding power supply in a co-evaporation process. A mobile shutter placed in close proximity to the substrate holder was used for avoiding the film formation before steady state evaporation conditions were obtained. Constant evaporation rates are necessary for obtaining a well-defined compositional gradient in multiple source co-deposition geometries.

All thin film depositions were carried out at room temperature in a pressure of 2×10^{-3} Pa and the temperature increase of the substrate due to radiation was below 20 °C at the end of the deposition. The distance between source and substrate was kept constant at 170 mm for all depositions. The thickness of the thin films was ranging between 150 and 450 nm, as measured using a contact profilometer (Dektak 3). The evaporation of the bulk Al–Cu alloy was done from a single source (W boat) with a rate of $1.0\,nm\,s^{-1}$ which required a power of 300 W. In the case of independently co-evaporating Al and Cu, the Al evaporation rate was fixed to $0.55\,nm\,s^{-1}$ (W boat) while the Cu source was stabilised at $1.0\,nm\,s^{-1}$ (5 mL Al_2O_3 crucible). Due to the geometry of the co-evaporation and the chosen rates, a compositional spread was obtained in this case across one set of substrates ranging from Al-57 at.% Cu to Al-93 at.% Cu. During this process, the electrical power necessary for the Al and Cu sources was 300 and 550 W, respectively.

Microstructural characterisation of all the thin films produced by co-evaporation was done using scanning electron microscope (SEM) and atomic force microscope (AFM) investigations. A field emission Zeiss Gemini 1540 XB SEM with 20 kV acceleration voltage and in-lens detection was used for the surface imaging. A Nanosurf easy scan 2 AFM operating in the contact mode was used for microstructural analysis. The crystallographic properties of

the Al–Cu thin film alloys were investigated using an X-ray diffraction (XRD) system (PANalytical X'pert Pro) using a Cu-K_α source. The compositions of the thin films were determined using the energy-dispersive X-ray spectroscopy (EDX) (Oxford INCA) technique. XPS depths profiling (ThermoFisher – Theta Probe) provided information about the in-depths chemical compositions of the samples. Electrical resistivities of the thin film alloys obtained from vapour phase depositions were measured using the van der Pauw method [20, 21]. This method was preferred due to the relatively small available area. Moreover, the sample holder used during the film formation led to irregular boundaries at the edges of the samples, which would complicate the interpretation of the results coming from the classical four point method. LabView software was developed for controlling the current applied to the investigated film surface through two contacts while measuring the potential difference on the other two. The current was increased in small steps of 0.001 A in order to monitor the resistivity changes due to the Joule effect.

3 Results and discussion In the present work, the fabrication and characterisation of Al–Cu thin film alloys is addressed. The properties of the thin films obtained from single or multiple sources are expected to differ due to the evaporation geometry which influences the dynamics of the vapour phase processes. During any physical vapour deposition process the thickness uniformity of the thin films formed is affected by the cosine of the incidence angle of the incoming species (θ) at different locations on the substrate. As a result, a thickness distribution defined by a cosine power function is always found and can be described as

$$\frac{d}{d_0} = \cos^{n+3}\theta, \tag{1}$$

where d_0 is the film thickness directly above the source ($\theta = 0$), while d is the thin film thickness at a specific location on the substrate defining the angle θ. The exponent n can be any positive number, and is zero only for the case of an ideal point source. Generally, the exponent of the cosine law (Eq. (1)) is greater than zero and it depends on the evaporand and the source geometry.

3.1 Co-evaporation of Al–Cu thin films For obtaining Al–Cu thin films during the co-evaporation process, individual Al and Cu sources were used. The effect of the cosine law (Eq. (1)) can be exploited during combinatorial thin film deposition by using two individual vapour sources creating two opposite concentration gradients [19]. After the co-deposition of Al and Cu, EDX analysis was used for mapping the compositional gradient along the surface of the entire sample set. These results are summarized in the 3D colour coded representation from Fig. 1. The Cu content of the Al–Cu compositional spread is plotted as a function of the position on the surface plane. The amount of Al is complementary for each experimental point as indicated by the equation presented in the inlet. A triangle-based interpolation method was used for fitting the experimental points measured in all 16 samples belonging to this set. For both, Cu and Al concentrations (Fig. 1) a gradient of 36 at.% was found. Directly above the Cu source at the sample position coordinates (−30, −30), 93 at.% Cu was measured together with complementary 7 at.% Al in the thin film alloy. This high amount of Cu is rapidly decreasing with the distance from the source, the lowest concentration of Cu (57 at.%) being found above the Al source at the position coordinates (30, 30). Here, 43 at.% of Al were measured in the Al–Cu thin film compositional spread. Along the direction perpendicular to the virtual line connecting the two sources, the same composition of the Al–Cu thin film alloys can be observed. This feature is present even though the overall thickness of the alloy thin film decreases due to the cosine law for evaporation (Eq. (1)). This compositional stability occurs due to the conservation of the ratio between Al and Cu during the evaporation when the individual evaporation rates are kept constant. Along the entire Al–Cu compositional spread an almost linear gradient was detected. This can be noticed in Fig. 1 by observing the approximately constant thickness of the coloured zones corresponding to each composition.

The microstructure of the Al–Cu thin films obtained by co-evaporation was investigated by SEM and AFM. In Fig. 2 the SEM imaging of the film surface is presented for several positions in the combinatorial library corresponding to different compositions. The Al-62 at.% Cu thin film alloy shows a smooth surface with uniformly distributed grains approximately 50 nm in size. Nevertheless, a low surface density of these grains can be observed while the areas between them are filled with much finer grains, which are close to the detection limit at the current magnification. Increasing the Cu concentration by 10 at.% resulted in a structural change of the Al–Cu thin films. The size of the grains increased to approximately 100 nm while their

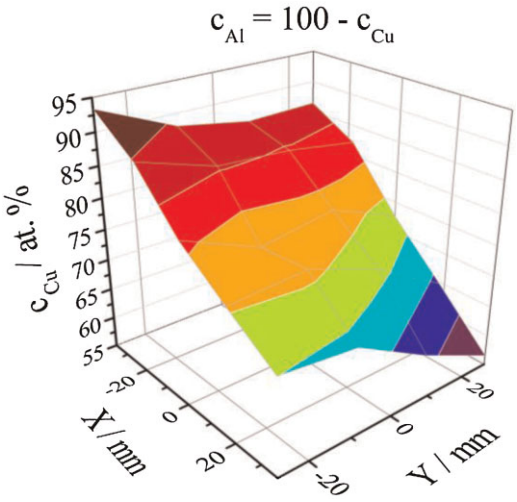

Figure 1 EDX of Al–Cu thin film compositional spread evaporated from two individual sources.

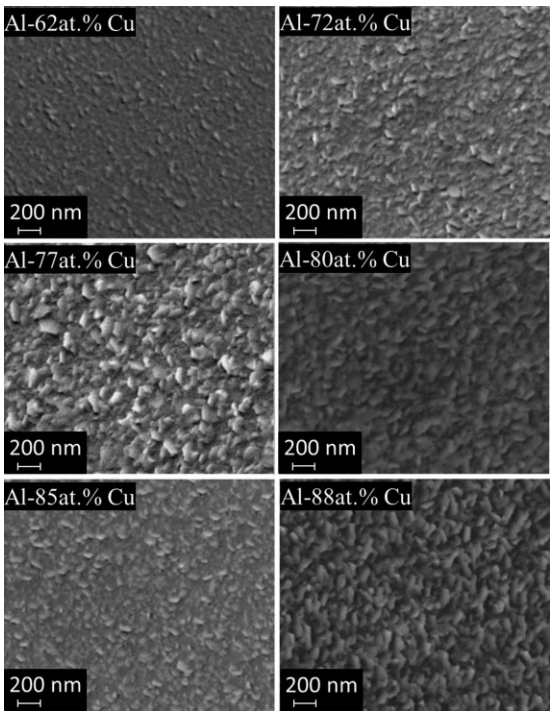

Figure 2 SEM image of Al–Cu thin film library evaporated from two sources.

shape became elongated forming a compact surface. Increasing even more the Cu content, the grains are evolving, their size continues to slowly increase until approximately 200 nm can be observed on Al-77 at.% Cu. At even higher Cu concentrations, the grain structure shows a more compact surface formed from elongated grains, which do not appear to considerably change with the composition.

In order to understand the microstructure evolution in the Al–Cu thin film combinatorial library, XRD investigations were systematically performed at various locations on the surface of the sample set. In Fig. 3, a compilation of XRD spectra is presented for the same compositions were the SEM

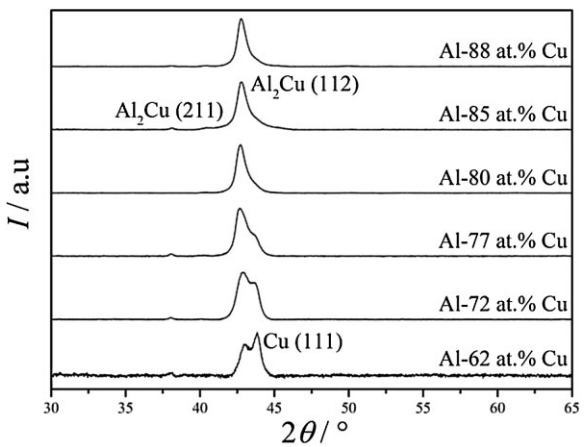

Figure 3 XRD results of Al–Cu thin films co-deposited from two different sources.

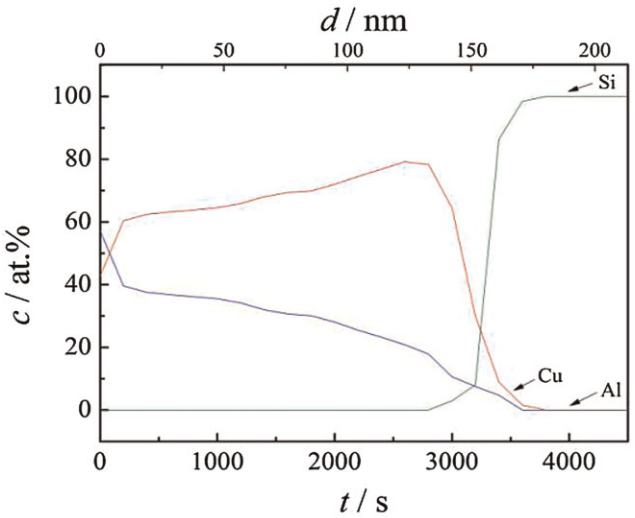

Figure 4 XPS depth profiles of Al–Cu thin films evaporated from two different sources.

analysis was performed. For all investigated cases, the presence of the Al_2Cu phase was detected and two diffraction peaks describing planes belonging to the same crystallographic family {112} can be observed. Additionally, the presence of Cu (111) can be seen for lower Cu concentrations in the compositional spread. Increasing the Cu amount, this peak decreases and starts being incorporated into the main Al_2Cu (112) peak, its detection becoming difficult. Moreover, the position of the Cu peak shifts towards lower angles with increasing the Cu amount, suggesting a continuous crystallographic change along the Al–Cu thin film combinatorial library. This behaviour may suggest that a pure Al_2Cu phase could be obtained at room temperature for high Cu concentrations. Similar results were recently found in Al–Cu alloys deposited by sputtering [16]. However, it was shown that the Al_2Cu phase is not forming above 100 °C, its stability being related to low temperature processing. The dynamic of the Cu peak can be related to the SEM results presented in Fig. 2. The strongest Cu (111) peak found on Al-62 at.% Cu coincides with the presence of a smoother surface observed for the same sample. This may suggest that the increasing amount of Cu along the sample set, associated with the stabilisation of the Al_2Cu phase, is responsible for the microstructure changes observed in the SEM investigations.

The composition of the Al–Cu thin films co-deposited from two independent sources was probed in depth by XPS. Using an Ar ion source, depth profiles were measured for the individual metallic components of the alloys. Additionally, the depth profile of Si was recorded in order to visualise the interface between the thin film alloys and glass substrates. In Fig. 4 a representative XPS depth profile measured on Al-66 at.% Cu thin film alloy is shown. The sputtering time given in seconds is presented on the horizontal axis. This can be related to the sample thickness (measured by contact profilometer) by measuring the location of the point of

inflexion in the Si profile where the amount of Si is increasing due to sputtering of the substrate. The corresponding sputtering time of approximately 7000 s describes a total thickness of 450 nm. A true depth scale is difficult to calculate since the composition slightly changes in-depth, leading to different sputter rates which affect the linearity of the depth scale. However, a depth scale was calculated and presented in Fig. 4 assuming that no significant compositional changes occur. Since the history of all samples within one set is identical, the in-depth chemical analysis for samples with different compositions is expected to show an identical trend. On the surface of the sample, no Cu could be detected in the depth profiles and the increased amount of Al is due to the presence of the naturally formed Al_2O_3. This was confirmed by separately measuring the O1s peak on the surface. Since the natural oxide on Al is amorphous, in the XRD results from Fig. 3 no peak was observed. The Cu amount is rapidly increasing with the depth in the first 500 s of the sputtering time, while the Al content decreases.

This suggests a surface segregation of the thin layer of alumina which protects the underlying alloy against further oxidation or chemical attack due to its self-inhibiting behaviour [22]. Starting from depths defined by at least 500 s sputter time, a positive deviation of approximately 15 at.% of the Cu concentration can be observed before reaching 2000 s while a negative deviation of approximately −10 at.% was found after 5000 s. Overall, both Al and Cu depth profiles show only slight variations around the composition of Al-66 at.% Cu measured by EDX.

The electrical properties of the Al–Cu thin film alloys were studied by means of measuring their electrical resistivity. van der Pauw method was applied for this analysis due to its advantages related to the sample geometry [23]. For this purpose each sample was electrically contacted at each corner using silver paste suspension. This ensured Ohmic contacting and each sample from the entire set was investigated. For avoiding temperature changes due to the associated Joule effect, the current was increased in small steps starting from low values (0.001 A). In this way, for no deviations from the linear current–voltage dependence were encountered (typical for a temperature change) for measurements up to 0.05 A. This makes a temperature independent measurement of the electrical resistivity across the entire library possible. Individual fitting of the current–voltage dependence (not shown here) allowed a direct calculation of the electrical resistivity. The results are presented in Fig. 5 as a 3D mapping of the electrical resistivity again as a function of the position within the sample set. Together with the experimental points clearly visible in Fig. 5, a wire frame surface was calculated using a triangle based interpolation method for fitting the results. The positions of the sources are identical with the ones presented before in Fig. 1. Directly above the Al source (30, 30) the resistivity of the alloys shows the highest values of approximately $2.2 \times 10^{-5}\,\Omega\,\mathrm{cm}$. Increasing the Cu amount, this value decreases by almost one order of magnitude, with values of approximately $8 \times 10^{-6}\,\Omega\,\mathrm{cm}$ being observable at the Cu rich side of the Al–Cu combinatorial library. The increase of the Cu content coincides with the enhancement of the Al_2Cu phase as shown in the XRD results from Fig. 3. This is to be expected due to the much better electrical conductivity of Cu as compared to Al. Similar to the case of the EDX presented in Fig. 1, on the direction perpendicular to the imaginary line connecting the Al and Cu sources no clear resistivity gradient was observed. This is due to the compositional conservation previously proven on this direction. Moreover, individual thickness values as measured by contact profilometry were used for calculating the electrical resistivity of each sample using the van der Pauw model.

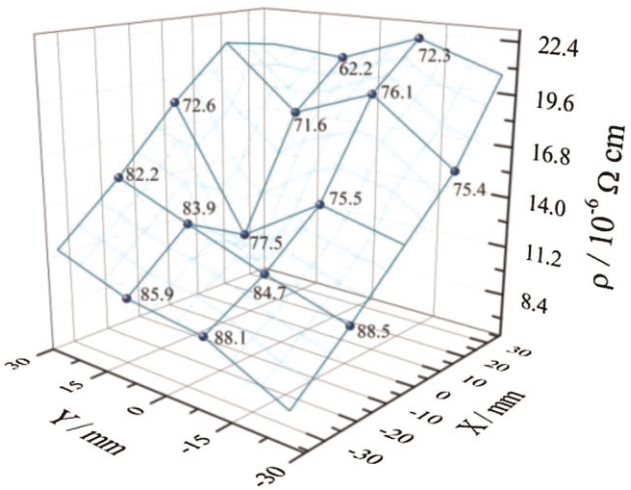

Figure 5 Electrical resistivity of Al–Cu thin films deposited from dual sources. The Cu content (at.%) is given for each point.

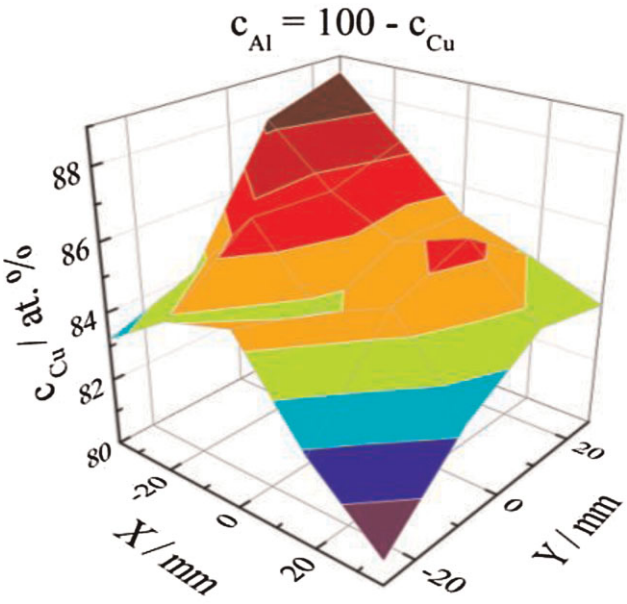

Figure 6 EDX of Al–Cu thin film alloys evaporated from a single sources.

3.2 Single source evaporation of Al–Cu thin films Al–Cu thin films were deposited using an Al-72 at.% Cu bulk source in the same conditions as the co-evaporation from individual sources. Due to the similar evaporation temperatures of Al and Cu (821 and 857 °C, respectively), evaporation from Al–Cu alloys is possible. This was proven by the successful Al–Cu thin film formation on glass substrates from a single Al–Cu source, which is addressed in this section.

The microstructure of the Al–Cu thin films obtained from a single source was investigated using SEM and AFM. However, due to the particularities of the films exhibiting no visible feature on the surface, SEM imaging was not possible. This normally suggests a very smooth surface. For measuring the surface roughness, contact mode AFM was used. Similar values were found for Al–Cu samples belonging to the set deposited using a single source. A much lower value of the root mean square (RMS) roughness was measured on Al–Cu thin films deposited from a single source as compared to the equivalent samples obtained from co-deposition using individual sources. The value of 5.2 nm was measured for the case of single source evaporation whereas the RMS roughness of the co-evaporation case was 30.5 nm.

In order to check the compositional uniformity of Al–Cu thin films obtained from a single source deposition, EDX measurements were performed. In Fig. 6 the results are presented as a 3D compositional spread and in this case the source position was (−30, 30). The 3D colour coded representation of the data was generated from fitting with a triangle-based interpolation method, similar with the previous EDX investigations from Fig. 1. A compositional gradient was detected ranging from approximately 88 at.% Cu down to 81 at.% Cu. Complementarily, the Al content ranged from 12 to 19 at.%. The higher amount of Cu was found directly above the source. Moving away from the source resulted in a slight decrease of the Cu content in the Al–Cu thin film alloys. This result is surprising since both, Al and Cu atoms are evaporated from the same source, therefore there is only one cos-law (Eq. (1)) corresponding to the Al-72 at.% Cu bulk alloy used as source. A single source should dictate a single cos-law and therefore a single thickness gradient. The interpretation of the present EDX data cannot be done solely based on Eq. (1) since this would require a second thickness gradient opposing the first one. As a result one must consider additional reasons for explaining the appearance of a compositional gradient in the Al–Cu thin film alloys deposited from a single source. For understanding this behaviour, a simple model can be used based on classical mechanics as traditionally used in gas phase dynamics. Since both Al and Cu atoms are released from the same alloy source they will have the same kinetic energy. The atomic mass ratio between Cu and Al is approximately 2.4 which defines a ratio between Al and Cu atom velocities of $\sqrt{2.4}$ with respect to the same kinetic energy. As a result, the Cu atoms will be able to deliver a momentum approximately 1.55 times higher than the Al atoms. During the vapour phase deposition, atomic collisions between Al and Cu must be considered and therefore the scattering probability of Al is higher than that of the Cu atoms. This could explain the enrichment of Cu directly above the source due to the shortest travel path to the substrate combined with the higher scattering of Al. As a result, Al will accumulate more in regions further away from the source given the extra kinetic energy received during collisions.

For investigating the in-depth film formation, XPS depth profiling was involved one more time. In Fig. 7 these results are presented as measured on a representative sample from the Al–Cu thin film sample set deposited using a single source. The etching time scale presented in the abscissa is directly related to the depths. Also in the case of using a single source for Al–Cu evaporation, an increased amount of Al is found on the surface. This is similar to the previously presented case of Al–Cu co-deposition, where Al_2O_3 forms on the surface protecting the alloy. A different trend was observed for the in-depth composition of the Al–Cu alloys deposited from a single source as compared with the ones co-deposited from individual sources. The amount of Cu is slightly increasing with the increase in etching time. The presence of more Cu closer to the film/substrate interface can be understood using the same mechanistic model presented in this section. The heavier Cu atom loses its energy more difficult than the Al atom and as a result it most likely has enough energy left for an in-depth segregation.

The electrical properties of Al–Cu thin film alloys deposited from a single source were investigated by measuring the electrical resistivity. In Fig. 8 the results obtained by using van der Pauw method for resistivity measurements are presented. The experimental points shown in a surface obtained using a triangle based interpolation method show a much smaller gradient as compared to the co-deposited samples. The highest electrical resistivity value of approximately $2.5 \times 10^{-5}\,\Omega\,\mathrm{cm}$ is comparable with the highest value measured on the Al–Cu compositional spread. The decrease of the Cu content above the source had as a result a decrease in the electrical resistivity and values as

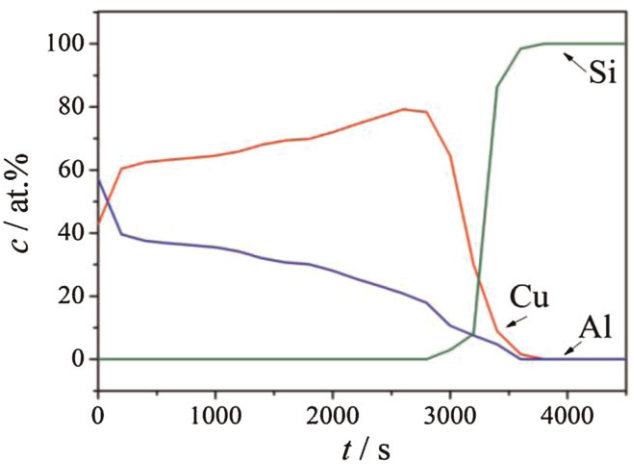

Figure 7 XPS depth profiles of Al–Cu thin film evaporated from a single source.

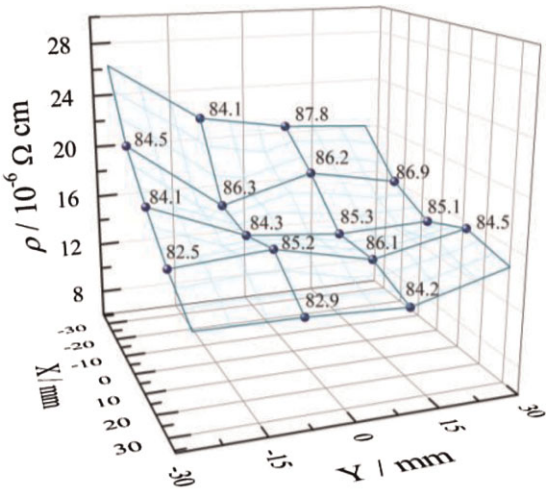

Figure 8 Electrical resistivity of Al–Cu thin films deposited from alloy source. The Cu content (at.%) is given for each point.

low as $1.2 \times 10^{-5}\,\Omega\,\mathrm{cm}$ were measured. However, due to the compositional limitation dictated by the single source evaporation, improved conductivities could not be reached.

4 Conclusions In the present work, the fabrication and characterisation of Al–Cu thin film alloys was addressed. Thin films obtained using a co-deposition geometry from individual Al and Cu sources were characterised. A compositional gradient ranging from 36 to 93 at.% Cu was obtained. Microstructural studies showed a strong influence of the Cu content on the surface evolution. These results were connected to the presence of the Cu(111) peak observed in the crystallographic studies. The electrical resistivity's measured using van der Pauw method showed a decrease by almost one order of magnitude in the Cu rich region of the Al–Cu combinatorial library. Al–Cu thin films evaporated from a single source were investigated and their properties were compared with the films obtained using a co-evaporation geometry. A surface compositional gradient (7 at.%) as well as an in-depth compositional gradient were found for the single source case. This behaviour was attributed to the gas phase dynamics of Al and Cu during the deposition. As compared to the case of co-evaporation geometry, the use of an Al–Cu alloy as a single source has a clear advantage of being straight forward while good stoichiometric reproducibility was demonstrated. Nevertheless, desired Al–Cu compositional spreads can be tuned only using two independent single element sources.

References

[1] F. Kobayashi, A. Nomura, and T. Kano, Electron. Commun. Jpn. **79**, 76–85 (1996).
[2] H. Qiu, F. Wang, P. Wu, L. Pan, L. Li, L. Xiong, and Y. Tian, Thin Solid Films **414**, 150–153 (2002).
[3] C. Y. Chang and R. W. Vook, J. Vac. Sci. Technol. A **9**, 559–562 (1991).
[4] B. Cao Martin, C. J. Tracy, J. W. Mayer, and L. E. Hendrickson, Thin Solid Films **271**, 64–68 (1995).
[5] A. Gladkikh, Y. Lereah, E. Glickman, M. Karpovski, A. Palevski, and J. Schubert, Appl. Phys. Lett. **66**, 1214–1215 (1995).
[6] A. J. Patrinos and J. A. Schwarz, Thin Solid Films **196**, 47–63 (1990).
[7] C.-K. Hu, R. Rosenberg, and K. Y. Lee, Appl. Phys. Lett. **74**, 2945–2947 (1999).
[8] W. Zhang, L. Yi, P. Chang, and J. Wu, Microelectron. Eng. **85**, 577–581 (2008).
[9] M. H. Lee, Y. M. Kwon, S. G. Pyo, H. C. Lee, J.-W. Han, and K.-W. Paik, Thin Solid Films **519**, 3906–3913 (2011).
[10] J. van der Kloet, A. W. Hassel, and M. Stratmann, Z. Phys. Chem. **219**, 1505–1518. (2005).
[11] S. O. Klemm, J. P. Kollender, and A. W. Hassel, Corros. Sci. **53**, 1–6 (2011).
[12] P. Phuku, P. Bertrand, and Y. de Puydt, Thin Solid Films **200**, 263–274 (1990).
[13] A. I. Mardare, M. Kaltenbrunner, N. S. Sariciftci, S. Bauer, and A. W. Hassel, Phys. Status Solidi A **209**, 813–818 (2012).
[14] M. Kaltenbrunner, P. Stadler, R. Schwödiauer, A. W. Hassel, N. S. Sariciftci, and S. Bauer, Adv. Mater. **23**, 4892–4896 (2011).
[15] F. Macionczyk and W. Brückner, J. Appl. Phys. **86**, 4922–4929 (1999).
[16] C. M. Su, H. G. Bohn, K. H. Robrock, and W. Schilling, J. Appl. Phys. **70**, 2086–2093 (1991).
[17] A. I. Oliva, J. E. Corona, and V. Sosa, Mater. Charact. **61**, 696–702 (2012).
[18] F. Haidara, M.-C. Record, B. Duployer, and D. Mangelinck, Surf. Coat. Technol. **206**, 3851–3856 (2012).
[19] A. I. Mardare, A. P. Yadav, A. D. Wieck, M. Stratmann, and A. W. Hassel, Sci. Technol. Adv. Mater. **9**, 035009 (2008).
[20] L. J. van der Pauw, Philips Res. Rep. **13**, 1–9 (1958).
[21] A. A. Ramadan, R. D. Gould, and A. Ashour, Thin Solid Films **239**, 272275 (1994).
[22] K. Schwabe, Angew. Chem. Int. Ed. **5**, 185–197 (1996).
[23] D. W. Koon, Rev. Sci. Instrum. **60**, 271–274 (1989).

